CSI RD&D (Solicitation 4) Subtask 4.2 Final Report:

Allocation of Battery Energy Storage Systems in Distribution Networks Considering High PV Penetration

Submitted to:

California Public Utilities Commission
California Solar Initiative RD&D Program

January 2016

Submitted by:

Oytun Babacan, William Torre, Jan Kleissl

Department of Mechanical and Aerospace Engineering
Jacobs School of Engineering
Center for Renewable Resource Integration and Center for Energy Research
University of California, San Diego
9500 Gilman Drive
La Jolla, CA 92093-0411

ABSTRACT

The question of how energy storage can be used efficiently and effectively in distribution networks is open and ongoing. This work proposes a methodology for optimal allocation of utility-scale battery energy storage systems (BESS) on the utility network to maximize their support for integrating high penetration solar photovoltaics (PV) in distribution networks and minimize cost.

A genetic algorithm (GA)-based multi-layer multi-objective optimization model is developed that minimizes the voltage deviation caused by high PV penetration and decreases energy loss in the distribution system while also accounting for the BESS capital cost and operational life expectancy. The optimization problem considers BESS unit capacities, BESS installation locations, and the cumulative BESS capacity of the network as decision variables. While construction limitations, environmental, and aesthetic impacts are not included in the present model, the algorithm could easily be modified to consider siting constraints that would play a practical role in resource allocation.

The effectiveness of the proposed method is shown with a benchmarking studies conducted on the IEEE 8500-Node test feeder. An additional case study is presented using a feeder in the SDG&E service area to demonstrate its applicability on real distribution feeders.

TABLE OF CONTENTS

I. INTRODUCTION 1
- A. Background 1
- B. Literature Review 1
- C. Scope of the Report 1

II. METHODOLOGY 2
- A. Problem Definition 2
  - Reducing Energy Losses in the Feeder, $L\Delta E$ 2
  - Mitigating Voltage Deviations at PV Generation Points, $Vdev$ 3
  - Evaluation of Battery Degradation, T 4
  - Assessing the Performance of the Investment, $\lambda cost$ 5
- B. Implementation of Battery Dispatch 7
  - Initialization 9
  - Power Flow Simulations 9
- C. Test Circuit, PV Penetration, and Data Sources 10

III. NUMERICAL RESULTS 11
- A. Results for a Sample Day 11
- B. Examples for the Progression of the Genetic Algorithm Optimization for Siting and Sizing 12
- C. Progression of Voltage Deviation 15
- D. BESS Siting 16
  - Additional Value Streams of Optimal BESS Configurations 18

IV. CONCLUSIONS 20

I. INTRODUCTION

A. Background

Planning and managing the electric distribution system is becoming more challenging due in part to the emergence of widespread distributed renewable generation. A less predictable generator may lead to a variety of issues, ranging from sub-optimal financial planning to unreliable operation. Considering that in the near future the rooftop solar photovoltaic (PV) systems will likely to saturate in low-voltage distribution grids, grid reinforcement may be required to keep the energy network running without operational issues and allowing further increase in PV penetration.

In a low-voltage distribution grid with high amounts of grid-connected solar PV, high generation and low load conditions are expected nearly on a daily basis when there is plenty of sunshine during midday but not many customers at home that require electricity. Such conditions may result in overvoltage events in parts of the grid and overload transformers and current carrying cables. Fluctuating electrical power during partial cloud cover may result in increased tap changes to compensate the resulting voltage fluctuations. A grid that is properly configured to host high amounts of PV systems is still prone to periods of thick cloud cover or rain that require high power flows from the substation to replace the missing local PV generation. In the absence of on-site storage, such events may be responsible for peak feeder loading. Such dependency will prohibit saving costs through capacity deferral. As a result, increased penetration of intermittent distributed power generation sources creates a great potential to investigate and implement storage technologies in distribution grids.

B. Literature Review

Real power injections from PV systems raise the voltages in a distribution grid. This increase depends on the amount of solar generation at that particular time, on the grid topology and on the node where the injection is happening [1]. Due to the temporal mismatch between peak solar PV generation and residential peak demand, power quality issues such as overvoltage at nodes with PV systems and instances of reverse power flow are likely to be observed in low-voltage distribution grids [2]. Other commonly impacts caused by high PV penetration can include the following:

- Voltage fluctuations due to intermittency of local power injections.
- Overloading of distribution circuits due to real / reactive power injection balance.
- Inability to maintain voltage regulation within Conservation Voltage Requirements (CVR)

Distributed storage is often considered as a viable tool to offset these impacts caused by distributed grid-connected solar photovoltaic systems. Utility-scale storage systems such as compressed air, flywheels, or batteries have been studied for decades and can be used for a wide range of grid services such as frequency control [3], network voltage control [4] and peak shaving [5].

Optimal operation and allocation of energy storage systems have been studied in the literature looking for an optimal trade-off between technical and economic goals. These studies introduce problem definitions that usually focus on one or several of the following categories: storage operation [5] - [6], storage sizing [7] - [8], and storage siting [9] - [10]. Many of these studies provide solutions to undesirable consequences arising from transforming the existing electric system with distributed renewable energy resources.

C. Scope of the Report

The motivation for this particular work is to understand the benefits of having energy storage systems in distribution networks with high PV penetration. A particular interest is to fill the gap in understanding how battery energy storage system (BESS) sizing and siting maximize the benefit of such systems. This effort often requires a problem definition that considers all three categories (storage operation, storage sizing, and storage siting) listed above.

This work formulates a genetic algorithm (GA)-based multi-layer multi-objective optimization model that optimally allocates BESS (storage sizing, storage siting) in a distribution feeder according to a storage dispatch strategy obtained from a linear programming (LP) routine (storage operation).

This paper is organized as follows: Section II introduces the methodology by providing a description of the objective function and its terms, the constraints and the implementation of the optimization routine. Section III presents the case studies with numerical results along with the data sources and the test circuit. Section IV concludes the paper with final remarks on the method.

II. METHODOLOGY

A. Problem Definition

The goal is to optimally size and site BESS within a distribution network under a certain penetration of distributed PV. The optimum BESS configuration is determined by the program by controlling the three decision variables: the size of each BESS, the installation node of each BESS, and the total BESS capacity in the feeder. The term *BESS configuration* is used herein to mean the set of these three decision variables.

The multi-objective optimization, given in Eq. 1, is formulated as a weighted sum method.

$$max\ \{[n_1\bar{L}_{\Delta E} + n_2\bar{V}_{dev} + n_3\bar{T}] \cdot \lambda_{cost}\} \qquad \textbf{1}$$

The optimization routine aims to maximize this relation. The terms given within the parenthesis represent various value streams for the utility that are defined in more detail in the following sections. In short, $\bar{L}_{\Delta E}$ is the energy loss reduction achieved through BESS utilization, $\bar{V}_{dev}$ is the reduction in voltage deviations at the most-impacted nodes within the network, and $\bar{T}$ is the overall operational life expectancy of BESS installed in the network. λ_{cost} is a penalty multiplier that accounts for battery procurement costs.

There are many other possible value streams that can be considered in the optimization formulation. The formulation shown in Eq. 1 aims to reduce distribution feeder voltage issues and energy losses through ideal BESS configurations while keeping BESS operation lifetime at acceptable levels. Other value streams could be added to this formulation and/or the physical parameters could be converted to economic value streams, but this would require knowledge of local conditions. The source code of the optimization is provided to permit others to customize the optimization.

The two perhaps most significant additional value streams are voltage regulation lifetime and capacity deferral. Voltage regulation lifetime is implicitly considered through the voltage deviation parameter as generally less voltage deviations implies less voltage regulator actions. Capacity deferral is implicitly considered by virtue of operating the batteries for peak shaving. The impacts of the optimized battery siting and operation are discussed in Section III.E.

The numerical value of this formulation is to be called the *fitness value* of a BESS configuration. All terms are normalized by an appropriate quantity so that values they assume fall in a similar range with comparable impact on the fitness value. Throughout this study each weight is always set to unity. Different weighting coefficients could be used in order to favor a certain value stream over others but results indicate that the present normalization is well-balanced and effective as formulated.

Reducing Energy Losses in the Feeder, $\bar{L}_{\Delta E}$

The energy loss in a distribution feeder P_L increases as customer demand peaks primarily due to increasing thermal loading in the conductors. Without any distributed generation in the network the peak energy loss is generally observed during the peak load (Figure 1a). As PV penetration (the ratio of installed PV capacity over rated feeder load) increases, required power supply from the substation during peak solar hours decreases and hence PV systems tend to reduce network energy loss at low to medium PV penetration during daytime. However, as PV penetration increases further, more local electricity is generated than actually needed and reverse power flow occurs (Figure 1b). As the amount of the reverse power flow increases, the energy loss in the network also increases. BESSs can shift PV generation from peak solar power generation hours to peak load hours, reducing congestion and energy loss and avoiding reverse power flows (Figure 1c).

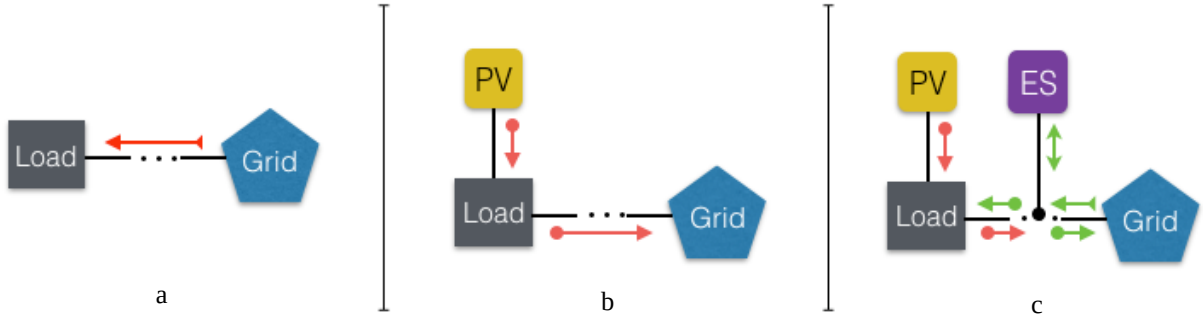

Figure 1. (a) Line congestion during peak load, (b) reverse power flow during peak PV generation and (c) utilization of energy storage to mitigate these issues.

The energy loss reduction $\bar{L}_{\Delta E}$ achieved through prescribed BESS scheduling is expressed in Eq. 2.

$$\bar{L}_{\Delta E} = \frac{\sum_{i=1}^{T}(P_{L,i}^{base} - P_{L,i}^{pv+bess})}{\sum_{i=1}^{T}(P_{L,i}^{base} - P_{L,i}^{pv})} - 1 = \frac{\sum_{i=1}^{T}\Delta P_{L,i}^{pv+bess}}{\sum_{i=1}^{T}\Delta P_{L,i}^{pv}} - 1 \qquad \mathbf{2}$$

The superscripts *base*, *pv*, and *pv+bess* indicate separate power flow simulation results – using the base circuit without PV systems or BESS, the circuit with PV systems, and the circuit with PV systems and BESS, respectively. Energy loss for each case in the entire network, ΔP_L, is determined by subtracting the *pv* and *pv+bess* cases from the *base* case for each time step $i = 1, \ldots, T$. The BESS fitness component is the ratio of these two differences. Since the ratio nears unity for nonoperational BESSs, the ratio is then normalized by subtracting one. In this way Eq. 2 does not contribute any positive value to the objective function if the BESSs are not operational.

Mitigating Voltage Deviations at PV Generation Points, $\bar{V}_{dev}$

Voltage deviations are caused by local variation in PV generation and/or demand. The inverters of the energy storage system can modulate reactive power and regulate voltage independent of the energy stored but this is not considered here. Specifics of how smart inverters will be allowed to inject reactive power for voltage control are still being worked out through standards working groups. UC San Diego is completing another CEC funded project with Sunspec Alliance to test the latest generation of smart inverters and ensure performance and compliance with California Rule 21 smart inverter and UL standards. It appears certain that smart inverters will improve voltage regulation and the impact of increasing renewable generation on voltage regulation will diminish in the future. An example of this control concept is demonstrated in Figure 12 (Section III). Energy storage systems can also decrease voltage deviations caused by local PV systems by absorbing the excess generation and discharging / supporting the network when the local generation decreases (e.g. due to a moving cloud impacting several PV systems).

From the PV case (no BESS), voltage variation caused by PV penetration are determined as

$$\Delta V = \sum_{n=1}^{N}\sum_{i=1}^{T}(V_{n,i}^{pv} - V_{n.i}^{ref}), \qquad \mathbf{3}$$

where the reference voltage $V^{ref} = 1$ p.u. independent of time (i's) or location (nodes n = 1, ..., N). The nodal voltage deviation ΔV across all nodes is then ranked based on per unit voltage difference (from highest to lowest). The top X number of nodes with the highest differences ΔV are selected as representative nodes. Here, X equals to the total number of installed PV systems in the network. Only these so-called *critical nodes* are considered in the network-wide metric so that the metric is not averaged out by less-effected nodes (typically located far from PV systems). This node filtering helps the optimization routine to site BESS in close proximity to the nodes with the largest voltage deviation.

The critical nodes are identified at each time step separately so that the voltage deviation metric updates itself to account for the most effected nodes at that time step. The voltage variance for the *pv* case ($V_{dev,i}^{pv}$) and the variance for *pv+bess* case ($V_{dev,i}^{pv+bess}$) are calculated at each timestep i at these critical nodes. The final metric for the cost function in Eq. 1 is then determined by taking the ratio of these two variances, subtracting one, and summing for each time step yielding the metric for the achieved voltage deviation reduction in the network by installing BESSs:

$$\bar{V}_{dev} = \sum_{i=1}^{T} \left(\frac{V_{dev,i}^{pv}}{V_{dev,i}^{pv+bess}} - 1 \right) \qquad \textbf{4}$$

Similar to the energy loss reduction $\bar{L}_{\Delta E}$ (Eq. 2), $\bar{V}_{dev}$ approaches zero for nonoperational BESSs.

Evaluation of Battery Degradation, $\bar{T}$

A simple battery degradation model is used to assess the impact of BESS operating strategies on BESS operational life expectancy (*BESS lifetime*). BESS lifetime acts as a differentiator between different BESS configurations with similar $\bar{L}_{\Delta E}$ and $\bar{V}_{dev}$ that are achieved with less impact on the battery.

A discharge event is defined as continuous power injections from BESS to the feeder that starts when BESS switches its operation mode from idling / charging to discharging and ends when BESS switches back to idling / charging mode from discharging. The total number of cycles the battery can endure for particular discharge event is assessed using Eq. 5 as proposed in [11].

$$L(x) = \left(\frac{u_o}{DOD}\right)^{u_1} e^{u_2 - u_3 DOD}, \qquad \textbf{5}$$

where DOD is the depth of discharge for a scheduled discharge event. The depth of discharge (DOD) is a measure of how much of energy is drawn out of the battery as a percent of the state of charge (SOC) of the battery. The DOD has a significant impact on the life expectancy of chemical battery energy storage. The parameters u_i are determined by performing a best fit of Eq. 5 to the cell cycle life data of a battery technology of interest as shown in Figure 2.

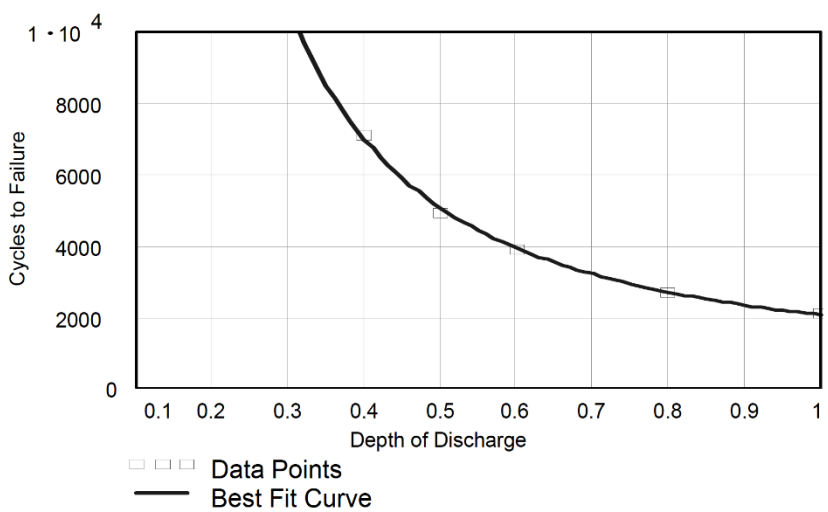

Figure 2. Best fit curve to manufacturer's cycle life data for pocket plate NiCd cells using Eq. 5 as reported in [11].

In this study, the reported values in [11] for Nickel-Cadmium (NiCd) batteries are used. The choice of battery technology was determined by the availability of public experimental data required to compute the parameters given in Eq. 5. The source code for the optimization is provided and any DOD and Cycles to Failure data can be considered in the formulated optimization routine once these data become available. Nevertheless, the reported typical cycle

lifetime for NiCd batteries are well within the range of the current market leader Lithium-Ion batteries (Table 1). In addition, several relevant charge and discharge characteristics of NiCd are also similar to other technologies listed in Table 1. Thus, the case studies shown in this study should be broadly representative of the most common battery technologies.

Table 1. Typical life time, discharge time, charge time and response time and self-discharge characteristics of different energy storage technologies. Reproduced from [12].

Parameter →	Typical Life Time	Typical Discharge Time	Recharge Time	Response Time	Self-Discharge
Technology ↓	Years (cycles)				%/day
Lead-acid	3-15 (2000)	min-h	8-16h	5-10ms	0.1-0.3
Nickel-cadmium	15-20 (2500)	s-h	1h	ms	0.2-0.6
Lithium-ion	8-15 (500-6000)	min-h	min-h	20ms-s	0.1-0.3
Zinc bromide flow	5-10 (300-1500)	s-10h	4h	<1ms	0-1
Vanadium redox flow	10-20 (13000)	s-10h	min	<1ms	0-10

The overall effect of cycling to a battery is determined using an event-oriented ageing model as described in [13]. Many distinct BESS operating schedules (i.e., discharge events) can occur based on local load and irradiance. Each scheduled discharge event *e* impacts battery lifetime differently and so they are considered separately as shown in Eq. 6,

$$LC_e = L(DOD_e)^{-1}, \qquad \textbf{6}$$

where DOD_e is DOD of a scheduled discharge event e and $L(DOD_e)$ is the corresponding estimated cycle life. In other words, LC_e captures the life impact, or "life cost", when BESS is operated at that particular DOD_e. The total operational cost of discharging $LC^{operation}$ is then calculated in Eq. 7 by summing the life cost of each event of schedule e on each BESS m.

$$LC^{operation} = \sum_{m=1}^{M} \left(\sum_{e=1}^{E} LC_e \right)_m \qquad 7$$

A battery reaches its end of lifetime when all its operational life costs sum to unity. The performance of a BESS is assessed based on the number days of similar operation it can endure until its end of lifetime as represented by $(LC_e{}^{operation})$^-1. The final step is to normalize the total number of days of sustained operation by a predicted or desired operational lifetime, T_{goal}, as shown in Eq. 8. T_{goal} in this study is chosen to be 10 years.

$$\bar{T} = \frac{LC_e{}^{operation^{-1}}}{T_{goal}} \qquad 8$$

Assessing the Performance of the Investment, λ_{cost}

An economic analysis of BESS typically requires consideration of capital, operating and maintenance costs [14]. While the objectives of this optimization routine (reducing energy loss and voltage deviation and prolonging BESS lifetime) could be monetized, decoupling the technical value streams of BESS from its economical value streams is beneficial at this stage, as costs are directly affected by non-technical and user-specific decisions or conditions (e.g. electricity rates, profit margins, interest rates, labor costs). Technical terms in the cost function allow the results to be reproduced and compared in different regions, while many of the monetization considerations will change significantly between utility territories due to distinct energy policies and market dynamics.

Following this idea, a qualitative BESS cost penalty model is applied that depicts BESS capital, installation and land-of-use, and economies of scale concepts and all costs are represented in the objective function as a single cost penalty multiplier, λ_{cost}, that penalizes larger capacity BESS (although partially mediated by reduced costs per unit) and more dispersed BESS installations in the network.

λ_{cost} is defined as

$$\lambda_{cost}(x_1, x_2) = \left(\frac{p_o}{x_1}\right)^{c_1} - c_1 p_1 (x_1 - p_o) - c_2 x_2, \qquad \textbf{9}$$

where p_o is the smallest permissible aggregated BESS size, p_1 is a scaling factor between the 1st and 2nd term of Eq. 9, c_1 is the sizing penalty constant, c_2 is the siting penalty constant. x_1 and x_2 are the variables of the optimization routine and represent the total installed BESS capacity in kWh and the total number of BESS sites in the network, respectively. The relation given in Eq. 9 is visualized in Figure 3 for p_o, p_1, c_1 and c_2 used in this study and the individual terms are discussed below.

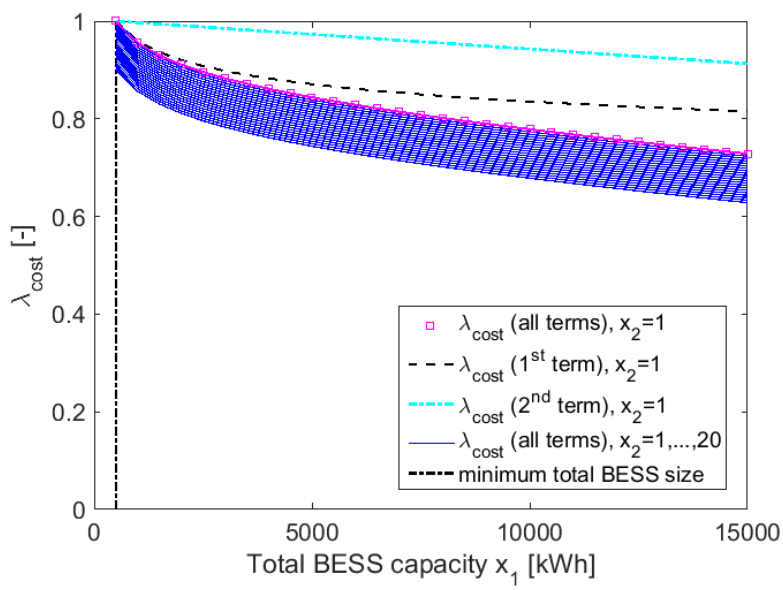

Figure 3. The cost penalty multiplier used throughout this study. (p_0 = 500kWh, p_1= 10^{-4}, c_1 = 0.060, c_2 = 0.005). The larger λ_{cost} the lower the cost. For this example graph, cumulative battery size (x_1) is varied between 0MWh and 15MWh, which is the typical range for the IEEE8500 simulations. The purple line shows the centralized case with a single BESS location (x_2 = 1) resulting in the lowest cost and neighboring parallel blue lines show increased penalty as the number of BESS installations (x_2) increases in the network. The black and cyan lines show the 1st and 2nd term of Eq. 9.

$\lambda_{cost}(x_1, x_2)$ scales the objective function in Eq. 1. It is maximized (lowest cost) when a centralized system (single BESS) is present in the network and the system has the smallest permissible aggregated BESS size ($x_1 = p_o$, $x_2 = 1$).

As x_1 increases, $\lambda_{cost}(x_1, x_2)$ decreases, reflecting the increasing capital cost of installing larger BESS (1st and 2nd terms in Eq. 9). Each additional BESS capacity δx_1 installed to an existing BESS configuration $x_1{}^*$ always decreases $\lambda_{cost}(x_1^* + \delta x_1, x_2)$. In this way, for the same conferred benefit, a cumulatively smaller BESS configuration is preferred in the optimization.

In current markets for bulk energy storage, economies of scale are difficult to ascertain due to the confidential nature of the emerging competitive market, large variations in the reported costs, and differing costs between different storage technologies accompanied with a lack of experimental performance data. Nevertheless, this model assumes that customers will eventually enjoy economies of scale for BESS implying a decreased marginal cost for every additional storage unit purchased from a vendor. The first term, $\left({}^{p_o}/_{x_1}\right)^{c_1}$, in Eq. 9 models economies of scale, i.e. as x_1

increases, the per unit cost is reduced. The second term ensures that per unit cost does not approach zero as x_1 increases (minimum cost per unit).

Another main consideration in the model is the number of BESS installation sites in the distribution network. For each additional BESS installation site the utility will incur additional fixed expenses (e.g. real estate, permitting, electrical interconnection). This relation is represented as a linearly increasing cost in Eq. 9 through the third term, $c_2 x_2$, that increases costs as more sites are used.

B. Implementation of Battery Dispatch

Batteries are chosen such that the kW rating of each BESS matches its kWh capacity (i.e. power to energy ratio of 1). Battery dispatch for each system is primarily determined by a linear programming (LP) routine that minimizes the daily non-coincident peak demand at the substation. The LP routine receives solar PV power and load forecasts as input and sets a net load reduction target. In principle, this target is adjusted throughout the day in response to forecast error. In this study, PV power and load data are provided to the LP routine as perfect forecasts, and consequently the battery dispatch is not affected by forecast error. For further detail about this routine see [5].

Perfect forecasts are an idealized assumption. In practice forecast errors in both load and solar power production exist. Given that geographic diversity on a distribution feeder is limited, especially solar forecast errors can be significant over the 24 hour timeframe associated with battery discharge scheduling. [5] Provides examples of impacts of forecast errors on battery dispatch. In our context, underforecasts of solar power would cause the BESS to charge prematurely potentially reaching 100% state of charge early in the day, at which point the BESS would be unable to absorb more solar generation e.g. in the afternoon which would lead to reverse power flow and overvoltages. Overforecasts of solar power would cause the batteries to charge too little during the day resulting in insufficient energy availability to shave the evening load peak. Overforecasts therefore reduce the ability to peak shave and cause undervoltages.

In practice the best approach to deal with these uncertainties is probabilistic modeling. Uncertainties of solar and load forecasts can be expressed through confidence intervals or probability distributions. Then these forecast uncertainties can be propagated to the cost function parameters. To implement uncertainty propagation, Monte-Carlo simulations could be run for every day with solar and load forecast inputs selected from a probability distribution. Based on the results the operator could choose a desired probability of exceedance (e.g. 5%) and the associated battery dispatch would be executed. Such a strategy would also require updating the battery schedule regularly during the day as the actual state-of-charge deviates from the modeled state-of-charge and as new forecast information becomes available. The exact implementation of such a probabilistic scheme in practice will be subjective due to operator risk profiles and target objectives of the battery siting and sizing. Therefore we assume perfect forecasts, but a probability method could be added to the source code as a wrapper around the present deterministic method.

Since reverse power flow can cause a variety of power quality and protection issues, the LP routine is adjusted. When there is a reverse power flow from the circuit to the slack bus, battery dispatch is updated to force the battery to charge for the duration of excess generation.

BESSs always start the day with 20% state of charge (their reserve energy) and return to that reserve energy at the end of the day. Thereby, no energy shift is allowed between different days for case studies that run multiple simulation dates.

The optimization routine is capable of restricting available installation nodes for potential BESS to any desired subset of the distribution network. Since the primary interest is utility-owned energy storage, the batteries are always located on medium voltage (MV) lines on the primary side of the load transformers. All other nodes are considered as a siting restriction.

Optimization method: Genetic Algorithms

Genetic Algorithm

Given the nonlinear nature of power flow analysis and fairly large and unknown solution space formed by the three decision variables and the battery dispatching strategy, genetic algorithms (GA) are a viable global search algorithm option for this problem. GA implementations are vast in literature and are proven to achieve near-optimality at low computational cost. The main consideration in GA implementation is setting up the right balance between *exploitation* and *exploration* concepts.

Exploitation indicates finding the best fitness value within a small subset of the solution space and is similar to 'hill-climbing' behavior of traditional gradient-based optimization algorithms. In contrast exploration is the effort for finding new hills in the complete solution space and is the main driver that keeps the optimization routine from getting

stuck to local minima. Favoring exploitation over exploration would likely result in premature convergence if the initialization set is not in the immediate vicinity of the optimal solution. Similarly, favoring exploration over exploitation would likely result in exhaustive computations and may also prevent the optimization routine from approaching the optimal solution altogether.

The general methodology in a typical GA is presented in Figure 4. After completing power flow simulations for each BESS configuration (*individual*) in the current set of simulations (current *generation*), the individuals are sorted with respect to their achieved fitness values. The best few individuals (*elite*) are directly passed to the next set of simulations (next *generation*) through *elitism*. This method (elitism) allows the optimization routine to keep the characteristics of good solutions. Preliminary simulations showed that an increased number of elites in the population did not contribute to better convergence characteristics unless the distribution feeder was subjected to high PV penetrations. Thus, only a single elite is passed to the next generation for PV penetrations below 50% in order to allow as many varying BESS configurations to be included in the simulation cycles. For PV penetrations higher than 50%, 10% of a generation is designated as elite.

Figure 4. Each new generation is created through Genetic Algorithm (GA) operators: selection, cross-over and mutation. The next generation includes best individual(s) from the current generation (through elitism) and newly created individuals as a result of GA operators.

After the elite are included in the next generation, the selection operator is executed. This operator randomly selects individuals from the current generation in order to form a *mating pool.* Depending on the preferred selection method, the chance of choosing an individual can be either directly or indirectly proportional to the fitness value of the individual. In our algorithm, a selection method called "tournament selection" is implemented. In this method, two random individuals are chosen from the current generation regardless of their achieved fitness value. Later on, a random number r is picked between 0 and 1. If this random number r is below the selection threshold k, (i.e. $r < k$) the fitter individual is added to the mating pool. Otherwise, (i.e. $r > k$) the less fit individual is included into the mating pool. If the selection threshold k is chosen to be greater than 0.5, fitter individuals are usually favored in the pool. This threshold is often called as *selection pressure* since it determines how often the genetic algorithm would choose fitter individuals over less fit individuals.

The cross-over operator is executed once the mating pool is formed through the selection operator. This operator creates diversity in the next generation. In our algorithm, a "parametrized uniform cross-over" method is used. In this method two individuals are chosen randomly from the mating pool regardless of their achieved fitness value. The goal is to create a new (*offspring*) individual out of these two (*parent*) individuals. In our application, for each permissible node in the distribution network, the method might result in one of the following results subject to a defined *swapping probability* p_s: the offspring has the same BESS unit as the first parent, or the same BESS unit as the second parent, or an in-between sized system compared to the parent units, and if both parents do not have a BESS system at a node, there is no chance of having a new BESS unit at that node.

Once the cross-over operator is executed, the next generation is almost complete. The remaining GA operator, mutation, ensures further diversity in the next generation. In this study, two different mutation operators are used. The first mutation operator, "mutation through random individual generation", is active in the beginning of the simulation and this operator simply introduces new randomly initialized individuals to the next generation. Preliminary

simulations showed that once the simulation is operated for a certain amount of generations, this operator no longer contributes to the diversity of the population as the average fitness achieved in the generation gets higher than any randomly generated individual can usually achieve.

A second mutation operator, "bit-string mutation", replaces the first operator after 15th generations. This operator randomly changes any BESS unit size and/or randomly installs or removes a BESS unit at any node. This method allows some individuals to have drastically different configurations in order to avoid the simulation from getting stuck at local minima in the solution space. Since this operator is highly disruptive (i.e. configurations are changed very significantly) to the existing solutions achieved so far, the mutation rate p_m for this operation is chosen to be small ($\boldsymbol{p_m = 10^{-5}}$). This mutation rate results in an average number of mutation per bits that is below 1bit/individual, which means on average it is unlikely for an individual to mutate. A statistical representation is given in Figure 5 for the impact of the mutation operator on total installed BESS capacity.

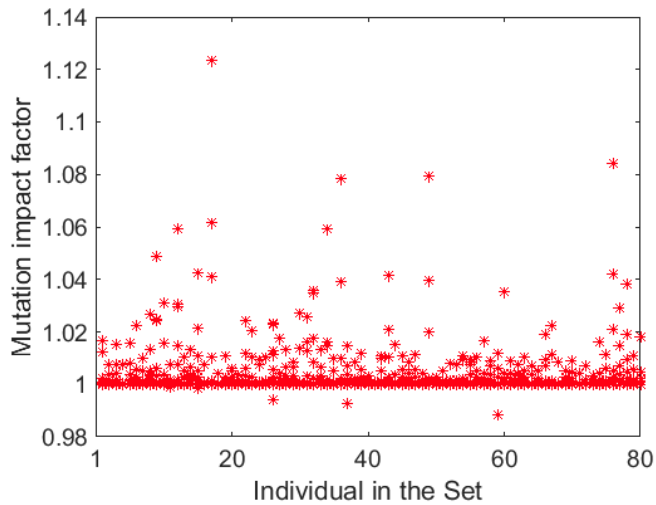

Figure 5. The change in total installed BESS capacity caused by the bit string mutation operator with a mutation rate of $p_m = 10^{-5}$ for a generation size of 80 individuals after running for 10^3 generations. *Mutation impact factor* indicates the BESS capacity scaling in upwards or downwards direction and is defined as the ratio of the total BESS capacity after mutations and the initial total BESS capacity before mutations.

Initialization

At the start of the optimization, 80 solution sets (*individuals*) are initialized. The number was empirically determined after running preliminary simulations comparing population sizes between 40 and 100, which are the recommended values reported in [15]. The results showed that the convergence of the optimization improves until 80 individuals and running simulation with even more individuals only increases computational cost. The individuals are initialized as follows:

- Randomly choosing a cumulative BESS kWh rating between a minimum permissible total size and the annual peak demand of the feeder. (The minimum permissible total size is taken as 500kWh.)
- Randomly choosing a number of BESS between 1 and 40.
- Randomly scaling the average BESS kW rating (the ratio of the cumulative BESS kWh rating and the total number of BESS) up or down.
- Random siting among permissible nodes.

Power Flow Simulations

Power flow simulations are performed using OpenDSS [16], an electric power distribution system simulator. The simulations have a time step of 15 minutes. The control mode for the solution is "static", indicating that the time does not advance and the control actions are taken in order of shortest time to act. The voltage regulators in the circuit are always set to regulate voltage between 0.95pu and 1.05pu with 0.01pu bandwidth. At each generation, OpenDSS simulations for each BESS configuration are run for a clear day, partly cloudy day and overcast day. The objective

function is calculated for each day and a fitness value for the individual is then determined by multiplying each day's result with its weather modifier (see Section II.D) and summing into a single fitness value. After assigning a single fitness value to each individual, the whole generation undergoes the GA operators: selection, crossover and mutation. This study uses tournament selection operator with a threshold value 0.60 and parameterized uniform crossover with a 0.75 swapping probability. In each generation three new randomly generated individuals are introduced to the solution set as the first mutation operator. The second mutation operator uses a mutation possibility of 10^{-5}.

While the initial conditions restrict the maximum number of BESS to 40 and the maximum cumulative BESS size to the annual peak demand of the feeder as described above, the optimization routine itself does not restrict the rating or the number of BESS that might be installed in the feeder. If favorable, the solution space may expand into larger and more dispersed system configurations compared to the initialization.

Reverse power flow is not allowed at the slack bus and BESS are scheduled to absorb excess generation. If a BESS configuration does not have the proper sizing to store this excess generation, it is discarded from the solution set. If a simulation for a BESS configuration does not converge or control iterations for the simulation are exhausted, this BESS configuration is discarded and a randomly generated BESS configuration is initialized and simulated instead. The initialization boundaries for these new BESS configurations are set based on the minimum and maximum total BESS size and BESS number of the individuals in the previous generation.

C. Test Circuit, PV Penetration, and Data Sources

The IEEE 8500-Node test feeder with balanced 120V secondary loads on the service transformers is chosen as the benchmarking circuit. This circuit is a radial distribution feeder with multiple feeder regulators and capacitors [17] and is a suitable test feeder to assess the performance of the proposed algorithm as it is similar to a large feeder with many typical elements found in a residential distribution feeder. Another case study is conducted for a distribution feeder in the SDG&E service area (*feeder E*).

The PV generation fleet is assumed to be composed of distributed rooftop systems located in direct proximity (i.e. secondary side of the service transformer) of respective load points. In the IEEE8500 feeder, for each level of PV penetration (up to 100% PV penetration), PV systems are sited randomly among the load points of the circuit until the desired penetration is reached. Each system is specified to have a capacity equal to the peak demand of that bus. For the *feeder E*, existing PV systems are kept in place while additional systems are added to the circuit at random locations. The specifications of these systems are assigned by randomly choosing a real system specification from a list formed by all existing systems in the feeder. Unlike for the IEEE8500 feeder case, the PV system locations are fixed and only the sizing for all PV systems is scaled to match the desired PV penetration.

Testing and demonstration of the algorithm is carried out using 15-minute resolution demand and solar generation data. For the IEEE8500 feeder, generic demand profiles for residential buildings in San Diego are imported from the data sets provided by Open Energy Information (OpenEI) [18]. PV power output data from 2014 are collected from six real PV systems located at the campus of University of California, San Diego campus. The PV system tilt angles are 10° and 20° depending on the system and their azimuth angle is 180°. Days representative of clear, cloudy and overcast conditions are chosen for the pool of days that are to be simulated. For the purposes of weighting each day in the overall cost function (Eq. 1) a weather modifier is calculated by taking the fraction of occurrence of each condition during the year (w_{clear}= 0.448, w_{cloudy}= 0.384, $w_{overcast}$= 0.168). For the feeder E case, a measured substation demand profile is applied to all load points. Solar generation is estimated using a ground-based sky imager [19] located within the feeder. The results are presented for 19th December 2012, a partly cloudy day. The weather multiplier in this case is taken as 1.

III. NUMERICAL RESULTS

A. Results for a Sample Day

In order to determine the BESS dispatch schedule for a simulation day and PV penetration level, power flow simulations are conducted using the *pv* case without including any BESS in the feeder. Total network demand and solar generation profiles are then supplied to the LP routine to determine the proper BESS dispatch for the simulation day and the level of PV penetration. Typical daily BESS operation is shown in Figure 6a and Figure 6b. This example shows a cloudy day with many ramp events in the IEEE feeder with 50% PV penetration.

The BESS smooth the ramps with short discharge cycles between 9am and 1pm. Without BESS reverse power flow through the slack bus would have occurred at 11:45am and at 1pm. Reverse power flow is mitigated by sending steep charging signals at these time steps. Prior to 6pm the BESS are fully charged and after 6pm are discharged to shave peak demand.

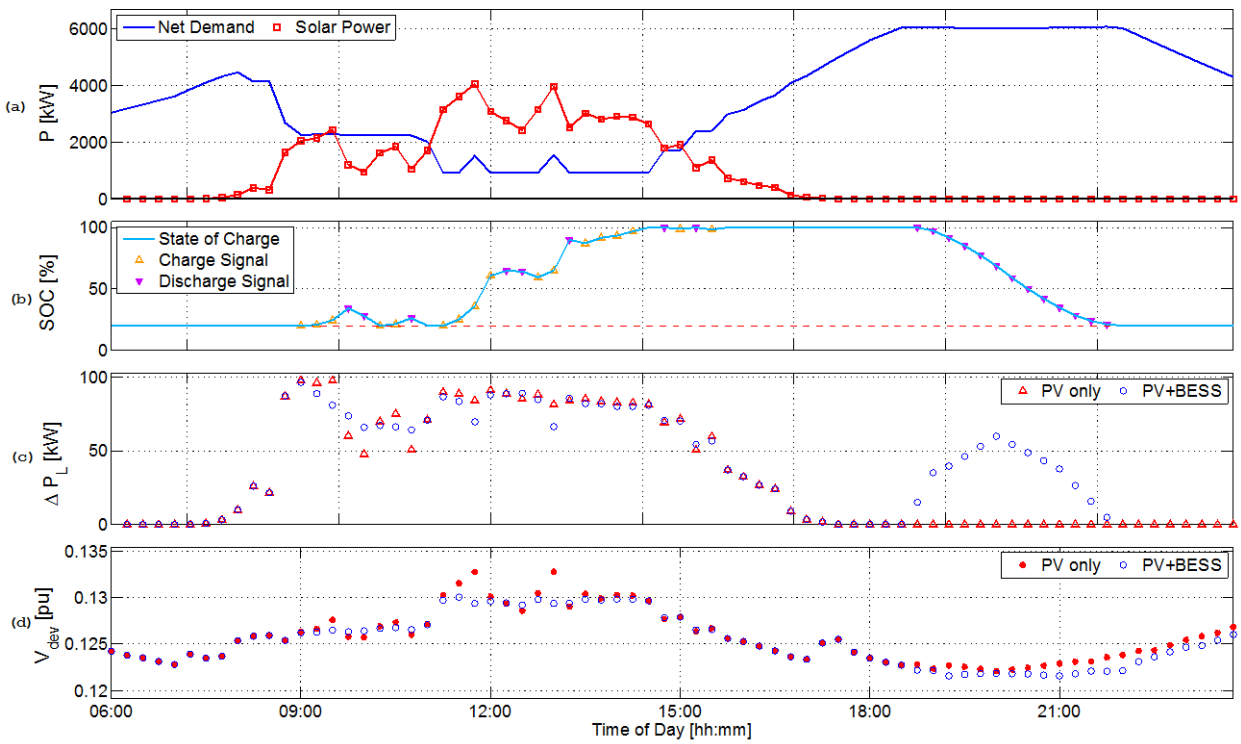

Figure 6. Overview of a typical daily simulation. The case shown is 50% PV penetration on a partly cloudy day (February 4th, 2014) (a) aggregate net demand (Load minus PV minus BESS) and solar power generation. (b) cumulative BESS state of charge and charging & discharging signals. (c) Energy loss reduction compared to the reference case (no PV). (d) voltage deviation among critical nodes with respect to 1pu.

From each power flow simulation, the benefit terms of the objective function in Eq. 1 are computed. Figure 6c shows the impact of PV ($\Delta P_{L,i}^{pv}$) and PV+BESS ($\Delta P_{L,i}^{pv+bess}$) operation on energy loss reduction for each time step i. During hours of PV generation, PV systems decrease energy loss since demand consumes locally-generated power. The BESS minimally increase energy loss because they charge, thereby adding to the feeder load. During the evening peak, the BESS dispatch and reduce energy loss significantly.

Figure 6d shows the impact of PV ($V_{dev,i}^{pv}$) and PV+BESS ($V_{dev,i}^{pv+bess}$) operation on voltage deviation for each time step i. Here BESS dispatch reduces net demand fluctuations caused by PV generation stabilizing the local voltage. BESS also support the voltage by injecting power locally during peak consumption. While the largest total reduction in voltage deviation occurs during the evening peak load, the largest temporary reduction occur during peak solar generation.

Battery degradation is quantified as described in Section II.A.d to calculate the impact of each discharge event shown in Figure 6b.

The objective function result is obtained from Eq. 1. If the simulation is conducted for a single day, this value is used as the fitness value for the genetic algorithm operators described in Section IIB. The individual with a particular BESS configuration is assessed by this fitness value as it undergoes each operator. If simulations include multiple simulation days, the fitness value is calculated by scaling each objective function result according to its weather multiplier as described in Section IID and summing into a single fitness value.

B. Examples for the Progression of the Genetic Algorithm Optimization for Siting and Sizing

Convergence properties of the GA simulations are illustrated in this section for the same day and penetration level as in Figure 6, i.e. 50% PV penetration on Feb 4, 2014, the partly cloudy day. Figure 7 shows the progression of total BESS size and number of BESS for all individuals during the complete duration of a simulation. The individuals initially show a great variety of BESS configurations covering a wide range of total BESS size and number of BESS. The variety of the later generations decreases as the optimization routine systematically favors BESS configurations with higher fitness values.

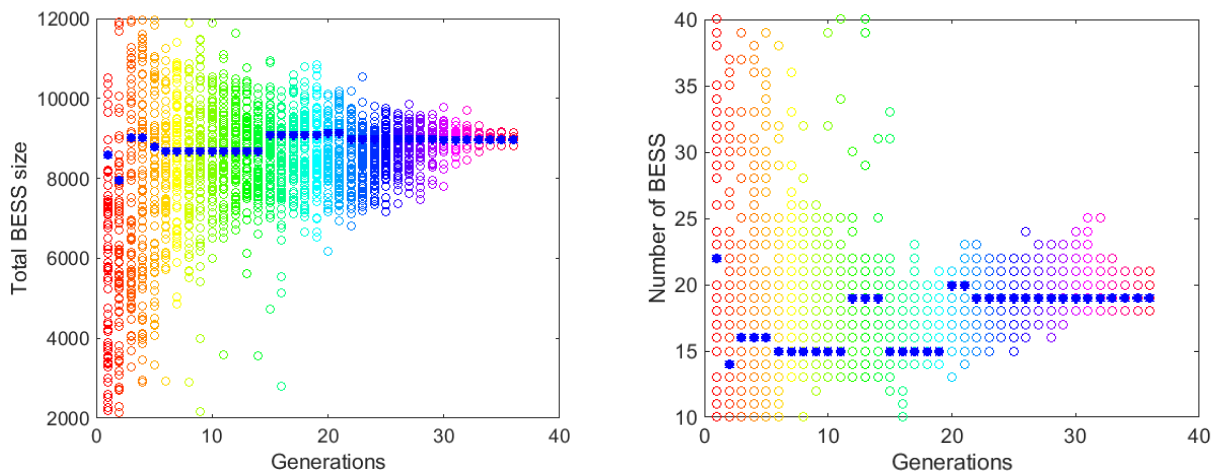

Figure 7. Results for the IEEE8500 test feeder simulation with 50% PV penetration for February 4th, 2014 (a partly cloudy day). The value marked with a blue dot shows the best BESS configuration achieved within each generation. All individuals of one generation are plotted superposed, e.g. individuals of the first generation (#1) are all given in x=1. Early generations including the initialization set are marked with red colors. The y-axis for each figure is slightly curtailed to exclude extreme values for better visualization.

The systematic search of the solution space conducted by the optimization routine is illustrated in Figure 8. The optimization starts its search with a wide coverage of the solution space. As the simulation progresses, the optimization routine increasingly focuses on exploiting the certain region of the solution space with the largest fitness values while still exploring other regions mainly by the means of random search through the mutation operator. The threshold parameters set for the genetic algorithm operators and the range of the initialization set determine the balance between this so-called *exploitation* and *exploration* behavior of the genetic algorithm.

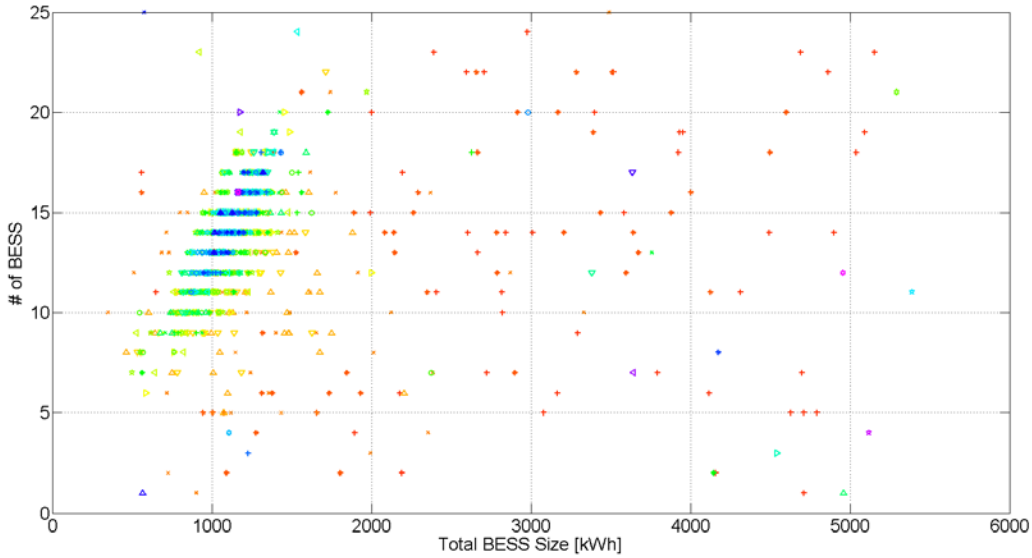

Figure 8. The progression of the total number of BESS and the total BESS size of each individual during a simulation with 25% PV penetration on a partly cloudy day (February 4th, 2014) executed for 30 generations. The individuals are initialized with a maximum number of 25 BESS and a maximum cumulative size of 6MWh. The color coding follows similar progression of generations shown in Figure 7.

It is important to note that Figure 8 does not explicitly show two of the decision variables: the installation nodes and unit BESS sizes. Each data point shown in Figure 8 might have a different composition of unit BESS sizes and locations.

Convergence characteristics of the optimization routine are shown in Figure 9 for the IEEE8500 simulations. Convergence is robust if different simulation runs result in the same maximum fitness achieved. The initialization sets are independently created at the start of each simulation run and are associated with fitness between 1.34 and 1.4**.** The termination criteria for convergence during these simulations is when the maximum fitness does not change by 0.005 for 15 consecutive generations. The mean optimized fitness of the group of simulations is 1.437. The maximum fitness difference for the converged solutions excluding outliers (the maximum and the minimum fitness achieved of the group) is 0.009 indicating that each simulation is likely close to the optimal solution.

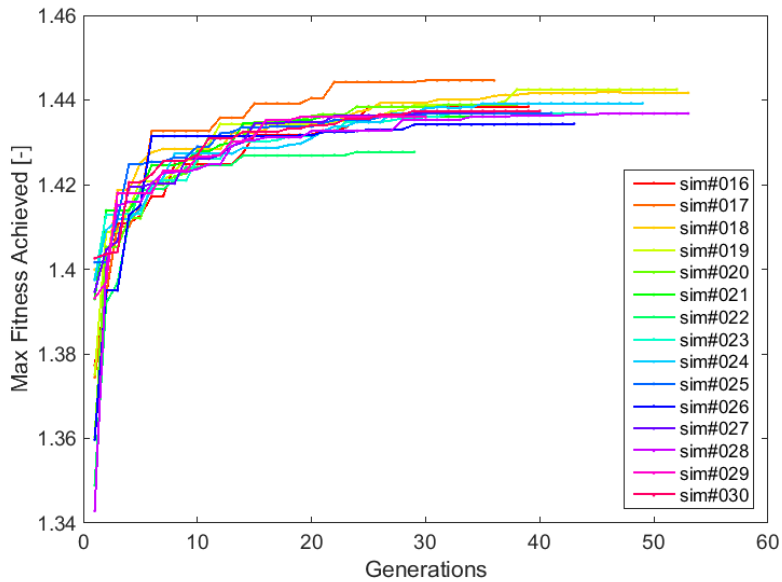

Sim #	Max. Fitness
16	1.438
17	1.445
18	1.442
19	1.443
20	1.439
21	1.436
22	1.428
23	1.437
24	1.439
25	1.437
26	1.434
27	1.437
28	1.437
29	1.436
30	1.437

Figure 9. The maximum achieved fitness values and progression of maximum achieved fitness values for 15 single day simulations that are independently initialized from each other. (IEEE8500 feeder with 50% PV penetration for February 4th, 2014)

Figure 10 shows the progression of total BESS size among the best individual of each generation for the same group of simulations as in Figure 9. This visualization shows the convergence for BESS sizing during the optimization. The total BESS capacity among all converged solutions differ by less than 1370 kWh and 87% of simulations differ by less than 280 kWh. It is important to note that 500 kWh is the smallest permissible BESS size. Similar successful sizing convergence is achieved among all simulations.

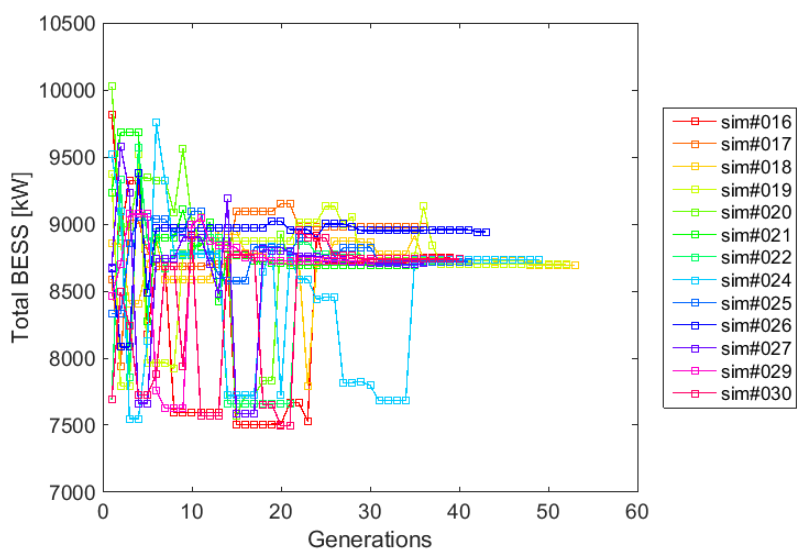

Figure 10. Progression of total BESS size installed among the best individuals of each generation for 15 simulations that are independently initialized from each other. (IEEE8500 feeder with 50% PV penetration for February 4th, 2014)

C. Progression of Voltage Deviation

Figure 11 illustrates how the voltage deviation sequentially improves within a single optimization run. In this figure, a decreasing marginal benefit in voltage with increasing installed BESS capacity in the network is observed. The polynomial fit approximates the maximum voltage deviation reduction $\bar{V}_{dev}$ at each BESS capacity. As the critical nodes in the network are supported with sufficiently sized BESS, additional BESS capacity cannot benefit the network with a similar impact. This eventually limits the total BESS capacity installed in the network as additional BESS cannot justify their additional marginal cost imposed by the cost penalty multiplier.

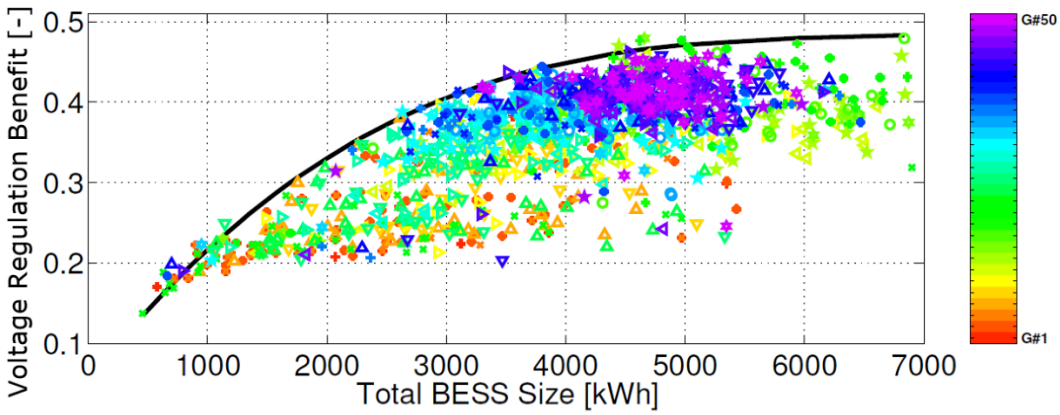

Figure 11. Voltage deviation metric $\bar{V}_{dev}$ (see Eq. 4 for definition) on the *y* axis versus total BESS size. Data are for the IEEE8500 feeder with 50% PV penetration. Results of individuals belonging to different generations are marked with different colors. The polynomial fit in black depicts the decreasing marginal benefit as the total BESS size increases. $\bar{V}_{dev}$ increases with improved voltage as the standard deviation of the voltage with PV only is divided by the standard deviation of the voltage with PV and BESS.

Historically, the IEEE Standard 1547 prevented distributed resources from actively regulating the voltage at their point of common coupling. Therefore, the optimization implemented in this study only considers voltage regulation with real power injection or absorption. However, IEEE 1547 is being revised to allow remote voltage regulation as part of smart inverter standard reform. Volt/var control can then provide local voltage support and offset the voltage deviations caused by distributed generation. To evaluate the impact of inverter Volt/Var control on voltage deviations, a Volt/Var management scheme was implemented as shown in Figure 12a for a sample feeder configuration. Without BESS, turning on Volt/Var control does not have a major impact on the voltage deviation metric (compare PV w/ Var and PV no Var). Therefore BESS still play an important function in voltage regulation on this feeder. However, the combination of BESS and PV Volt/Var control offers significant benefits for voltage. In this example, the voltage deviations in the evening peak load period when BESS inject power to the grid for peak shaving purposes could be mitigated through Volt/Var control. We note that the results presented here are likely suboptimal. The smart inverter Volt/Var curve and conventional utility voltage regulator settings would have to be coordinated to achieve the intended results. However, this analysis is beyond the scope of this report.

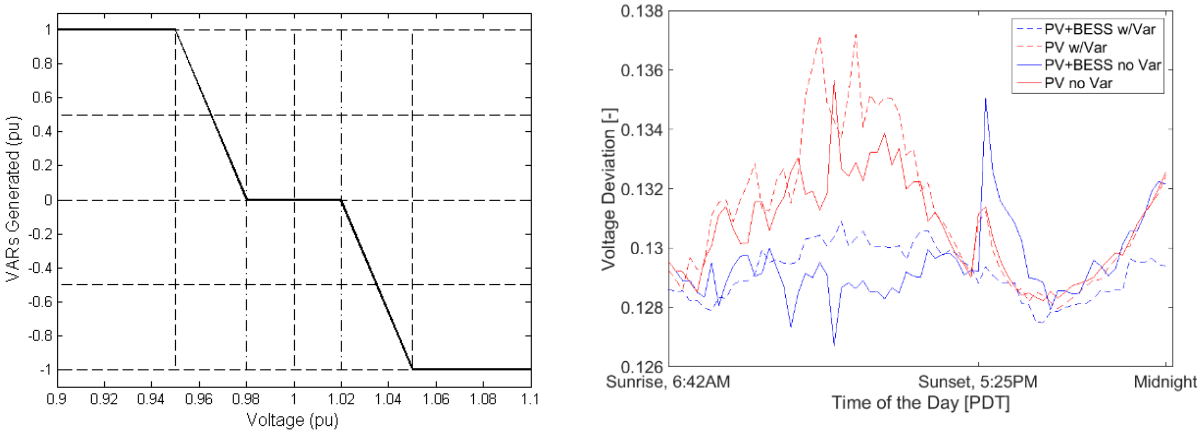

Figure 12. Demonstration of smart inverter Volt/Var control and its impact on voltage deviation. To force BESS charging with excess solar energy, BESS operation starts at sunrise. Left: Volt/Var Settings for PV inverters. Right: Voltage deviation (as defined in Eq. 3) for PV only and PV+BESS simulations with and without implementing smart PV inverter Volt/Var control. (Demonstrated on an optimal GA allocation configuration for IEEE8500 feeder with 50% PV penetration for February 16th, 2014)

D. BESS Siting

With regard to siting, there are three types of energy storage that are currently being installed in California: behind the meter, community energy storage, and bulk utility energy storage. Behind the meter energy storage is generally installed at a commercial-industrial or residential property and electrically connected behind the utility billing meter. Location and siting of behind the meter energy storage is not addressed in this study since utilities currently have little control over these the operation or placement of these systems.

Community energy storage is currently being installed and tested by all three major IOUs in California, and generally range in size from 20 – 100 kW. Community energy storage is generally installed directly within existing utility distribution easements and franchise right of way, and not in the substations, see Figure 13for examples of installations at San Diego Gas and Electric Co. Community energy storage is generally connected directly to distribution primary and secondary power lines. This report focuses primarily on siting of community energy storage systems along the distribution system to improve overall distribution system performance and reliability.

Figure 3 Left: 25 kW, 50 kWh community energy storage installed in franchise position along distribution circuit. Right: 25 kW, 25 kWh S&C Community Energy Storage System installed in distribution easement (photos courtesy of San Diego Gas & Electric Co.)

Bulk energy storage is generally located within utility substations and is used to improve both distribution and transmission system performance, and is aimed at improving resource adequacy in addition to system performance and reliability. This study does not specifically address optimal location of energy storage by restricting location to utility substations, but the proposed methodology could be adapted for this use. It is envisioned that a future study

will focus on the distribution and transmission system and address bulk energy storage location optimization at substation locations.

The siting decisions for optimally sized and dispersed BESS units are shown in 4 on a distribution feeder map. The circuit on the left is the original IEEE8500 circuit sketch reported in [17]. The substation, regulator and capacitor locations marked on the sketch are kept the same through this study. On the right side, a representative simulation result for 50% PV penetration is illustrated (note that as explained in Section X, the PV locations differ by penetration level).

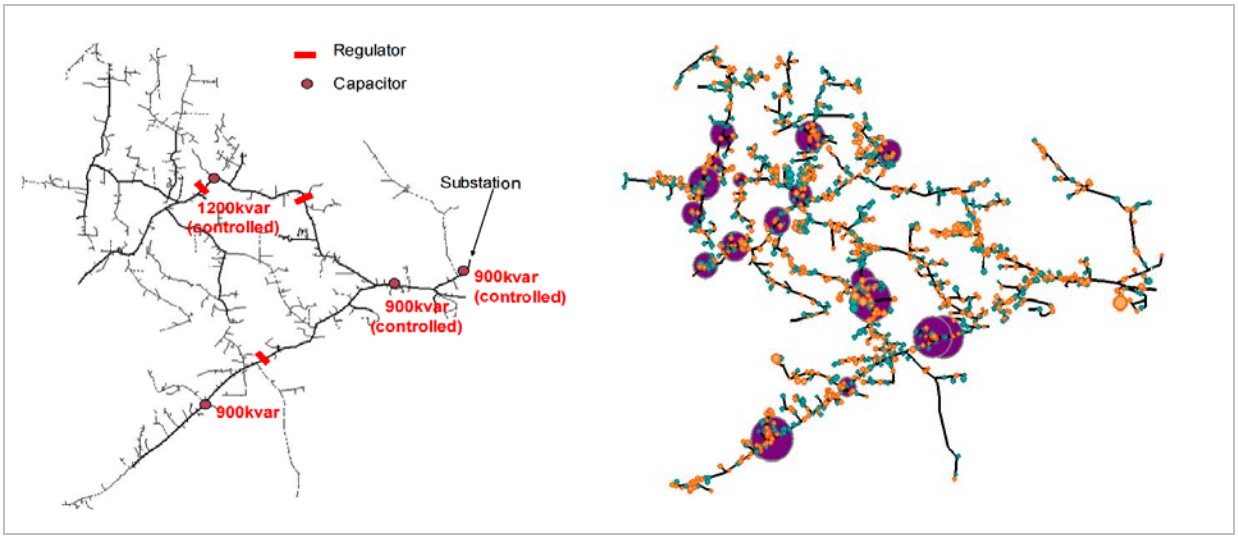

Figure 4. IEEE8500 test feeder one-line diagram and siting results of a representative simulation with 50% PV penetration for February 4th, 2014 (a partly cloudy day) (Left) One-line of IEEE8500 test feeder primary lines with the regulator and capacitor locations marked. This figure is originally printed in [17] and re-printed here. (Right) One-line of the optimal solution. Locations of proposed BESS units are marked with purple dots. Orange dots show loads with PV and turquoise dots show load points with no PV. Each dot is sized with respect to the capacity of the component it is representing.

Optimal solutions of three different simulations for the IEEE8500 test feeder and for the *feeder E* are given in Figure 15 and Figure 16, respectively. For each feeder, 6 different regions are marked with red circles. These circles identify regions where the optimization routine consistently sited one or several BESS with varying magnitudes. The number of these circles are chosen arbitrarily and they could be aggregated into fewer bigger circles.

The variation of BESS siting within these marked regions are natural and expected given the heuristic nature of the optimization routine and insignificant impact of re-locating certain BESS to their immediate neighboring nodes. However, identifying such regions with a degree of confidence is important to validate the methodology. Considering that there are 1177 permissible nodes on the primary lines for the IEEE8500 test feeder and 1621 permissible nodes on the lines for the *Feeder E*, convergence to several distinct regions within each circuit as demonstrated in Figure 15 and Figure 16 show that the optimization routine correctly implements the methodology presented in Section II and successfully recommends preferred locations for BESS to achieve utility objectives.

In summary, the permissible nodes for BESS installation points within the network can be tailored to account for any siting restrictions due to technical, environmental or human factors. The optimization routine accepts any subset of the network for BESS siting consideration and returns the feasible siting options and proper BESS sizing for the given permissible node set, demand and solar profiles, and the level of PV penetration in the circuit. The optimization routine will find the best location and size based on electrical system performance, however it is very probable that siting constraints, such as environmental, geographic, and others could make some locations infeasible.

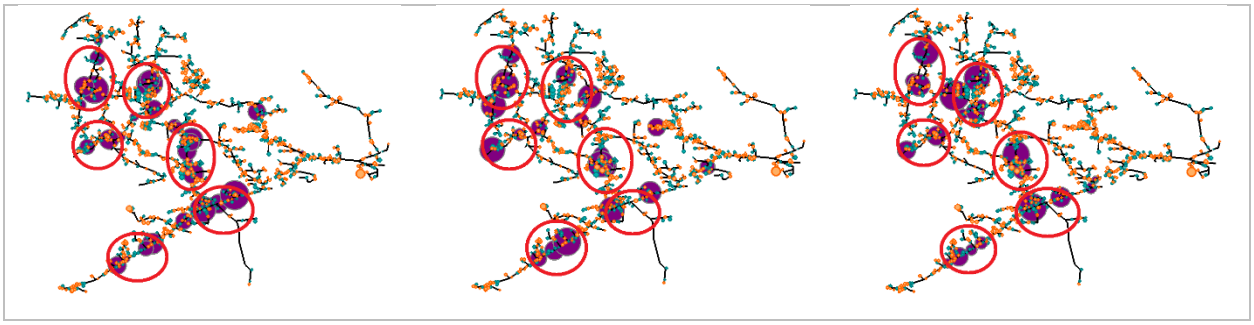

Figure 13. Optimal solutions of three different simulations for the IEEE8500 test feeder with 50% PV penetration for February 16th, 2014 (a partly cloudy day). Frequently chosen regions for BESS installations are marked with red circles.

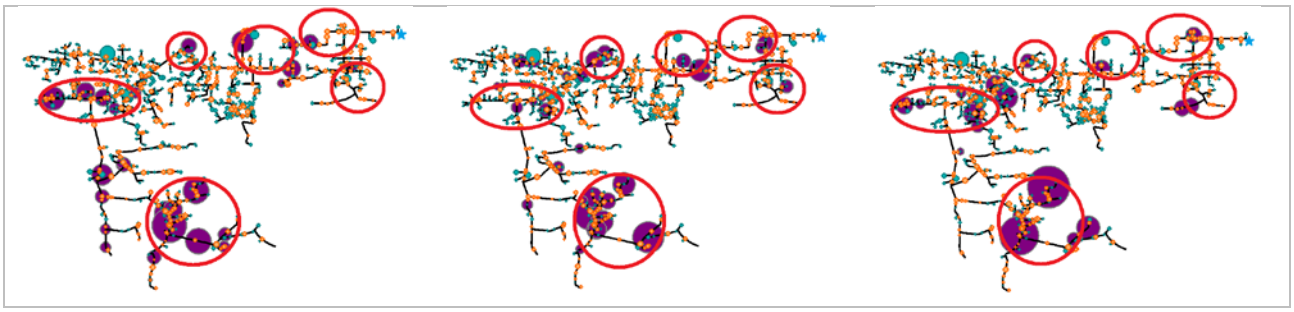

Figure 14. Optimal solutions of three different simulations for the *feeder E* with 75% PV penetration for December 19th, 2012 (a clear day with passing clouds in the evening). Frequently chosen regions for BESS installations are marked with red circles. The substation location for the feeder is indicated with a blue star on top right.

The optimization routine often places several BESSs in close proximity of each other as observed in one-line diagrams given above. The underlying reason for this placement scheme is due to the inter-connected permissible node set on the primary lines of the network. Such close placements will not occur if the permissible node set is chosen as discontinuous / isolated points within the network. If inter-connected permissible node sets are preferred, either closely placed systems can be aggregated into single systems as a post-processing step, or a minimum distance condition between each BESS can be imposed during the simulations.

Additional Value Streams of Optimal BESS Configurations

Economic value streams such as minimization of the peak load and BESS capacity, and reducing voltage regulator actions are implicit goals in the optimization through the voltage deviation reduction and cost reduction terms in the objective function, respectively. While value streams are not explicitly used in the optimization, they can be deduced in post-processing from the amount of peak shaving and voltage regulator actions observed in the simulations.

The peak power demand reduction in the distribution network is 36% from 6.66 MW to 4.23 MW. Assuming an average 2% load growth annually, this demand reduction would delay the need for a substation capacity upgrade by more than 15 years. This capacity deferral is well over the target BESS lifetime (10 years) assumed in this study. Additional capacity deferral benefits would accrue to specific line sections, but this would require a more detailed analysis.

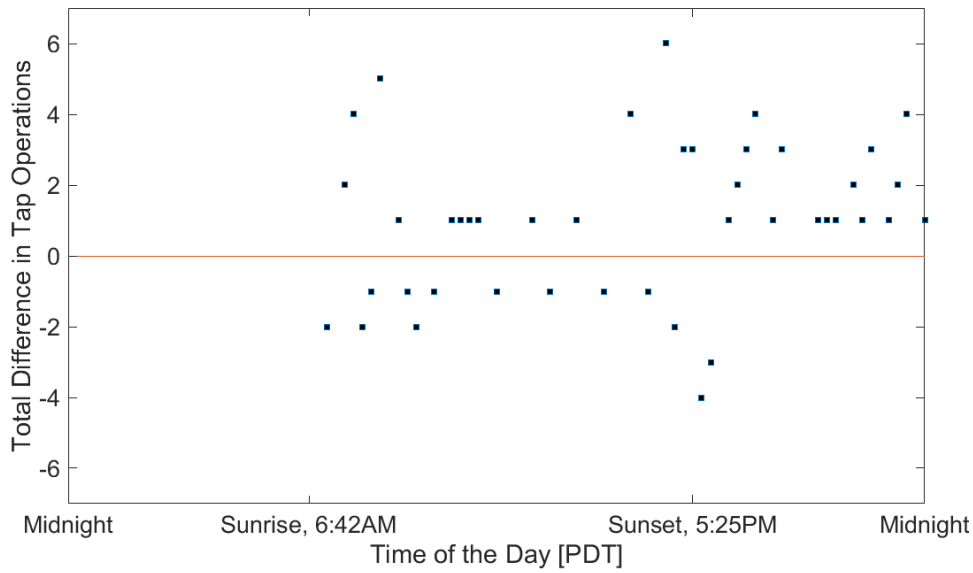

Figure 15. Difference in the total number of tap operations among all 4 voltage regulators in IEEE8500 between the PV only and PV+BESS cases. Positive difference means a reduction in tap operations with the support of BESS scheduling. (Demonstrated on an optimal GA allocation configuration for IEEE8500 feeder with 50% PV penetration for February 16th, 2014)

Another savings achieved through adoption of BESS in distribution systems with high PV penetration scenarios is reductions in tap operations of voltage regulators. As more and more PV systems are connected to the nodes in distribution networks, without ancillary forms of voltage support such as Volt/Var control, the utility voltage regulators are required to change tap position in order to keep the local voltage within the preset bounds of the operator. These actions, in return, diminish the lifetime of the equipment. As demonstrated in Figure 17, BESS can significantly decrease the amount of tap operations by the voltage regulators. In the case shown in Figure 17, 43 out of 147 tap operations (~29%) are eliminated through BESS scheduling. Assuming a linear relationship of regulator lifetime with tap operations, this reduction in tap operations would extend the equipment life to 1.41 times of the operational lifetime without BESS.

IV. CONCLUSIONS

The work presented in this report described a methodology for optimal allocation of utility-scale battery energy storage systems (BESS) to support high penetration solar photovoltaics (PV) integration in residential distribution networks. The developed model consists of a genetic algorithm (GA)-based multi-layer multi-objective optimization routine.

Benchmarking was carried out on the IEEE 8500-Node test feeder and the influence of initial conditions and GA settings are analyzed. BESS sizing and siting results were then computed for the IEEE 8500-Node test feeder and an actual California distribution feeder. The proposed method provides consistent solutions that appear to be optimal.

The permissible nodes for BESS installation points within the network can be tailored to account for any siting restrictions due to technical, environmental or human factors. The optimization routine accepts any subset of the network for BESS siting consideration and returns the feasible siting options and proper BESS sizing for the given permissible node set, demand and solar profiles, and the level of PV penetration in the circuit.

REFERENCES

[1] M. E. Baran, "Accommodating high PV penetration on distribution feeders," *IEEE Trans. Smart Grid,* vol. 3, no. 2, pp. 1039-1046, 2012.

[2] C. J. Bennett, R. A. Stewart and J. W. Lu, "Development of a three-phase battery energy storage scheduling and operation system for low voltage distribution networks," *Applied Energy,* vol. 146, pp. 122-134, 2015.

[3] P. Mercier, R. Cherkaoui and A. Oudalov, "Optimizing a battery energy storage system for frequency control application in an isolated power system," *IEEE Transactions on Power Systems,* vol. 24, 2009.

[4] M. Nick, R. Cherkaoui and M. Paolone, "Optimal allocation of dispersed energy storage systems in active distribution networks for energy balance and grid support," *IEEE Transactions on Power Systems,* vol. 29, 2014.

[5] R. Hanna, J. Kleissl, A. Nottrott and M. Ferry, "Energy dispatch schedule optimization for demand charge reduction using a photovoltaic-battery storage system with solar forecasting," *Solar Energy,* vol. 103, pp. 269-287, 2014.

[6] E. L. Ratnam, S. R. Weller and C. M. Kellett, "Scheduling residential battery storage with solar pv: Assessing the benefits of net metering," *Applied Energy ,* vol. 155, pp. 881-891, 2015.

[7] Y. V. Makarov, P. Du, M. C. W. Kintner-Meyer, C. Jin and H. F. Illian, "Sizing energy storage to accommodate high penetration of variable energy resources," *IEEE Transactions on Sustainable Energy,* vol. 3, 2012.

[8] Y. M. Atwa and E. F. El-Saadany, "Optimal allocation of ESS in distribution systems with a high penetration of wind energy," *IEEE Transactions of Power Systems,* vol. 25, 2010.

[9] M. Nick, M. Hohmann, R. Cherkaoui and M. Paolone, "On the optimal placement of distributed storage systems for voltage control in active distribution networks," 2012.

[10] G. Celli, S. Mocci, F. Pilo and M. Loddo, "Optimal integration of energy storage in distribution networks," 2009.

[11] S. Drouilhet and B. L. Johnson, "A battery life prediction method for hybrid power applications," 1997.

[12] K. Cavanagh and J. K. Ward, "Electrical energy storage: technology overview and applications. EP154168," CSIRO, 2015.

[13] D. U. Sauer and H. Wenzl, "Comparison of different approaches for lifetime prediction of electrochecmical systems - using lead-acid batteries as example," *Jounrla of Power Sources,* 2008.

[14] C. Chen, S. Duan, T. Cai, B. Liu and G. Hu, "Optimal allocation and economic analysis of energy storage system in microgrids," *IEEE Transactions on Power Electronics,* 2011.

[15] A. M. S. Zalzala and P. J. Fleming, Genetic Algorithms in Engineering Systems, IET, 1997.

[16] *Open Distribution System Simulator (OpenDSS),* Version 7.6.4.36 ed., Electric Power Research Institute.

[17] R. F. Arritt and R. C. Dugan, "The IEEE 8500 Node Test Feeder," 2010.

[18] "Commercial and residential hourly load profiles for all tmy3 locations in the United States," Office of Energy Efficiency Renewable Energy.

[19] H. Yang, B. Kurtz, D. Nguyen, B. Urquhart, C. W. Chow, M. Ghonima and J. Kleissl, "Solar irradiance forecasting using a ground-based sky imager developed at UC San Diego," *Solar Energy,* vol. 103, pp. 502-524, 2014.